Journal of Energy Storage 45 (2022) 103719

Contents lists available at ScienceDirect

Journal of Energy Storage

journal homepage: www.elsevier.com/locate/est

Research Papers

Towards the development of a novel bipolar-based battery in aqueous electrolyte: Evaluation of the electrochemical properties of NiCu based hydroxide electrodes fabricated on Ni–mesh and graphite composite current collectors

Dorcas Zide [a,b,*], Cecil Felix [b], Tobie Oosthuysen [a], Jens Burfeind [c], Anna Grevé [c], Bernard Jan Bladergroen [b]

[a] Department of Chemistry, Cape Peninsula University of Technology, Symphony Way, Bellville, Cape Town 7535, South Africa
[b] South African Institute for Advanced Materials Chemistry (SAIAMC), University of the Western Cape, Robert Sobukwe Road, Bellville, Cape Town 7535, South Africa
[c] Safety, and Energy Technology UMSICHT, Fraunhofer Institute for Environmental, Osterfelder Str. 3, Oberhausen DE-46047, Germany

ARTICLE INFO

Keywords:
Bipolar NiFe battery
Monopolar electrode
Graphite substrate
Ni-mesh substrate
Current collector
β-nickel copper hydroxide cathode
Iron-copper anode

ABSTRACT

The use of bipolar electrodes in rechargeable batteries can improve specific power, simplify cell design, and reduce manufacturing costs. However, bipolar-based batteries still suffer from many drawbacks. Therefore, developing high-performance active materials and developing improvement strategies encompassing the entire cell's design is essential. The current collector significantly impacts the viability of mass production; however, it is the most neglected feature of electrochemical energy storage devices. The current collector serves a dual purpose; it allows the movement of electrons among active electrode material and provides mechanical support. It can also act as transportation of current to terminals of the battery. This study constructed a novel bipolar battery cell utilizing graphite as a current collector, and its discharge capacities for Ni-Fe battery applications were evaluated. Monopolar NiFe cells, one using a graphite substrate current collector and the other using a Ni-mesh current collector, were used for comparison. The monopolar-based electrode coated onto a graphite substrate demonstrated a 29% (199 mAh/g) higher discharge capacity than the Ni-mesh-based electrode (142 mAh/g) after the 100th cycle. In contrast, the bipolar-based NiFe battery cell resulted in a discharge capacity of 158 mAh/g after the 100th cycle, corresponding to a coulombic efficiency of 72%.

1. Introduction

The assembling of bipolar batteries' knowledge originates at the initiation of electrochemical science from the voltaic pile battery [1]. The initial Pb-acid-based bipolar battery that utilized a pile of hallow-shaped electrodes dived by glass balls was patented by Tribelhorn in 1897 [1]. A maximum power density of 35 kW/kg was obtained by Kapitza in 1923 when he immersed a Pb plate in an electrolyte solution made of H_2SO_4 to contract a bipolar Pb-acid battery [1,2]. However, due to short-circuiting bipolar Pb-acid that employed liquid electrolytes went in vain. Since then, bipolar electrode designs have been introduced into the design of various battery chemistry technologies such as nickel-metal hydrides [3], Li-ion batteries and post-Li ion batteries, Li-S batteries [4], and Na-ion batteries [2,5–7]. Some researchers incorporate the bipolar plate design into alkaline batteries of Al and Zn metals as active electrode materials for high-power operation [8–10]. Golodnitsky and co-workers donated to the essential understanding and archetypal design utilizing the Li/CPE/FeS_2 batteries [11].

Currently, research scientists are investigating the technological drawbacks that hinder the advances of the bipolar construction [2, 12–14], which include (i) possible inner short-circuiting among cell units caused by the electrolyte, (ii) the possible bipolar plates decomposition vulnerability and (iii) complex cell stacking production progressions. Thus, developing high-performance active materials and developing strategies encompassing the entire cell's design is essential. The current collector is a commonly ignored constituent of electrochemical-based energy storage devices, which significantly impacts the viability of upscaling. The current collector serves a dual

* Corresponding author at: Department of Chemistry, Cape Peninsula University of Technology, Symphony Way, Bellville, Cape Town 7535, South Africa.
E-mail address: zided41@gmail.com (D. Zide).

https://doi.org/10.1016/j.est.2021.103719
Received 1 September 2021; Received in revised form 22 November 2021; Accepted 29 November 2021
Available online 6 December 2021

purpose; it allows the movement of electrons among active electrode material and provides mechanical support. It can also act as transportation of current to terminals of the battery. The current collector should have a relatively low-cost, high electrical conductivity, high mechanical strength, and good (electro) chemical stability in the electrolyte under various operating potentials to be suitable for profitable high-powered aqueous devices. Additionally, thin and lightweight current collectors are essential for the typical capacity and weight [15–19]. It is, however, challenging to design or select current collectors that simultaneously satisfy all or most of these critical requirements.

Carbon-based current collectors are firm over a broader scope of electrolytes and have many advantages over metals as current collectors [20]. The carbon current collector/electrode interface typically has lower contact resistance because of the passivating oxide film [21]. Due to large kinetic overpotentials, carbon can suppress hydrogen and oxygen evolution, improving electrochemical stability over a wider potential window in aqueous electrolytes [22]. Therefore, various carbon materials have been studied as current collectors. Although the use of carbon fibre, carbon nanotube papers, and mats have been explored as current collectors, these current collectors are porous, fragile, and not suitable for practical applications [2,15]. Various researchers have studied expanded graphite foils and have shown that it is ideal as current collectors for aqueous electrochemical energy storage [23–26].

In monopolar design, current collectors, also called monopolar plates, act as negative (anode) or positive (cathode) electrodes [12,14, 27-29]. These monopolar configurations are typically composed of a number of cells linked in a series by external wire, resulting in reduced gravimetric or volumetric energy density of a battery unit. Nevertheless, this increases the cost of material and intricacy of the battery. The advantages of a typical monopolar configuration include easy construction of unit cells in the presents of liquid-based electrolytes. The limitations are high power and high voltage applications owing to the external electrical connections causing increased resistance due to long electron pathways [14]. For example, on discharge, the electrons that move from the anode of one cell travels through the in-plane of the monopolar plate towards a negative terminal. Then, it moves via the outer wire towards the positive terminal of the next cell. Lastly, from the in-plain of the monopolar plate to enter the cathode.

The downsides of monopolar-based batteries encourage the development and evaluation of the bipolar-based electrode for Ni-Fe application. Contrary to monopolar design, external wiring is evaded in bipolar design, where the bipolar plate connects several cells in series. The exclusion of external wiring does not only gives an operative manner to mount and join the cells, but it also diminishes the electrical resistance, volume, weight, and cost of a typical bipolar-based battery [4,14]. Moreover, in a bipolar battery, anode and cathode materials are placed on opposite sides of a conductive substrate, which allows the through-plane movements of electrons to the next cell. The through-plane movement of electrons provides a quicker electrical pathway and a minimized power loss owing to the Ohmic drop in the circuit. Additionally, eradicating external circuit constituents like terminals, straps, and poles can reduce the volume of the battery [14,22].

This study prepared and evaluated a novel bipolar battery cell using a $Ni_{0.75}Cu_{0.25}(OH)_2$ cathode and a $FeCu_{0.25}$ anode with graphite composite as the current collector for Ni-Fe battery devices. Though the compactness of a bipolar battery configuration offers interesting advantages, it also poses some challenges. Charging and discharging parameters are applied over the entire stack without individual cell control and balancing, typically performed by a battery management system. This limitation requires robust electrode chemistry that is not sensitive to undercharge and overcharge conditions, rendering Li-ion battery chemistries less suitable in bipolar battery configuration. Ni-Fe batteries show some renewed interest in renewable energy applications due to their potentially long life, robust and durable qualities [30–32]. However, the Ni-Fe battery suffers from drawbacks such as low efficiency (50% - 60%) and low specific energy. Ni-Fe batteries are typically confined to stationary applications due to its heavy and bulky design; however, with the bipolar design and the use of a thermoplastic graphite composite bipolar plate, weight and size reductions may be achieved, extending the possible applications of Ni-Fe batteries.

In an attempt to mitigate the aforementioned downsides of Ni-Fe batteries, in our previous studies, the active materials for both the anode [33] and cathode [34–36] were optimized. A summary of our findings are as follows: Among different metal dopants (Mn^{2+} [36], Mg^{2+} [36], Co^{2+} [34], Al^{3+} [34] and Cu^{2+} [35] at different ratios (0.95:0.05; 0.9:0.1; 0.75:0.25 and 0.5:0.5) of Ni: metal dopants (Mn^{2+}, Mg^{2+}, Co^{2+}, Al^{3+} and Cu^{2+}) 0.75:0.25 Ni:Cu was found to be the optimal ratio and the best composition in terms of electrochemical performance as reported in our publications [34–36]. In one of our in-house studies [33], Fe electrode material was synthesized and evaluated for its electrochemical performance. The study utilized a combination of both Cu and FeS additives plus graphite particles. Briefly, FeS/C substituted Fe-Cu composite material was synthesized as anode material to be utilized in Fe-based alkaline batteries. The rationale behind this was that Cu should circumvent Fe particle agglomeration during cycling, graphite should formulate a good conductive network, subsequently improving the reversibility of the active material, and FeS should impede the parasitic hydrogen evolution reaction and the passivation process. The FeCu0.25/15%FeS/5%C electrode exhibited stable performances marked by high specific capacity coupled with negligible capacity decay and high efficiency.

In this work, we attempted to further improve the performance and practicality of the Ni-Fe battery by using a bipolar configuration. In this study, the polypropylene graphite sheets were developed and supplied by Fraunhofer UMSICHT, Germany. By using a heated multi-roll rolling mill and a compound of graphite, carbon black, and a thermoplastic elastomer, Fraunhofer UMSICHT has successfully manufactured a conductive and highly flexible bipolar plate in a continuous one-stage process [37]. When the roll size or welding of several sheets was used, the polypropylene graphite sheets could be manufactured in any size up to several square meters and current thicknesses down to 0.4 mm [37]. The manufactured polypropylene graphite sheets are gas-tight, chemical resistant, mechanically stable, and allow for a subsequent reshaping. The specification of as-prepared polypropylene graphite sheets by Fraunhofer UMSICHT [37] are summarized in Table 1.

DIN EN ISO 527-3 tensile tests have shown an elastic modulus of 1100 N/mm^2 as well as a tensile strength of 7.4 N/mm^2 at a strain of 1.6% and filling grade of 80% graphite and carbon black [37]. Depending on the carbon content, particle size, and morphology, the in-plane conductivity of the polypropylene graphite sheets ranges from 250 S/m up to 5000 S/m and exceeds the through-plane conductivity consistently by a factor ranging from 10 to 100 [37].

Currently, the authors could not find any literature reporting on a bipolar Ni-Fe battery. The results of this study are presented systematically. First, the electrochemical discharge capacities of two battery cells consisting of monopolar electrodes prepared with graphite composite film and Ni-mesh substrates as the current collectors, respectively, are evaluated and compared. In addition, a bipolar-based battery cell consisting of a bipolar electrode prepared with a graphite substrate as the current collector is assessed as a novel bipolar Ni-Fe battery. Advantages of using a standard bipolar-based electrode include but are not limited to improved specific power, simplify cell mechanisms, and reduce engineering costs aimed at secondary batteries.

2. Material and methods

2.1. Materials

The $Ni_{0.75}Cu_{0.25}(OH)_2$ material was synthesized using analytical grade materials, the in-house $FeCu_{0.25}$ was used as the anode electrode material [33]. Ni-mesh was obtained from Q-Lite Batteries in China, and the modified graphite substrate was obtained from Fraunhofer Umsicht

Table 1
Bipolar plate specifications (Sourced [37]).

Norm	Elastic modulus	Tensile strength	Filling grade		In-plane conductivity	Through-plane conductivity
DIN EN ISO 527–3	1100 N/mm^2	7.4 N/mm^2	80% Graphite	20% PP	250 S/m - 500 S/m (Depending on the carbon content, particle size, and morphology)	In-plane conductivity exceeds the through-plane conductivity consistently by a factor of 10 to 100

(Germany). Lithium monohydrate and potassium hydroxide were purchased from KIMIX (South Africa).

2.2. Synthesis of $Ni_{0.75}Cu_{0.25}(OH)_2$

The $Ni_{0.75}Cu_{0.25}(OH)_2$ material was prepared as explained by Zide and co-workers [35]. Briefly, a solution composed of NaOH and Na_2CO_3, and the second solution contained Ni^{2+} as $Ni(NO_3)_2{\cdot}6H_2O$ salt and Cu^{2+} as $Cu(NO_3)_2{\cdot}3H_2O$ salt were prepared. These solutions were titrated dropwise while continuously stirred at room temperature. The resulting slurry was aged further for 30 min, then hydrothermally treated at 65°C for 18h, cooled at room temperature, then sieved and splashed with Milli Q water. The final residues were then dried at 110°C for 12h.

2.3. Electrode Preparation

The $Ni_{0.75}Cu_{0.25}(OH)_2$ electrodes were fabricated by thoroughly mixing 85 wt.% active material, 10 wt.% Coathylene binder and 5 wt.% carbon black. The schematic diagram for the electrode production is shown in Fig. 1.

Briefly, the composite materials were hot-pressed onto a substrate (nickel mesh and graphite) using a custom-built hydraulic press with integrated hot plates (HyJack, Cape Town). The pressure of the hydraulic system was set at 6 MPa, which corresponds to 61.18 kgf/cm^2. The pressing process was started after the pressure plates reached 80℃. The compaction pressure on the sample was maintained for 5 min to ensure good electrical contact between the substrate and active material.

2.4. Galvanostatic capacity measurements

Galvanostatic capacity measurements were conducted in a two-electrode setup consisting of the in-house $FeCu_{0.25}$ anode and $Ni_{0.75}Cu_{0.25}(OH)_2$ cathode electrodes in a 6M KOH/1M LiOH electrolyte. The monopolar electrodes using Ni-mesh and graphite composite substrates were evaluated first for their discharge capacities. Subsequently, a bipolar cell consisted of a bipolar graphite composite electrode coupled with two Ni-mesh monopolar electrodes.

3. Results and Discussion

3.1. Structural characterization of $Ni_{0.75}Cu_{0.25}(OH)_2$

Fig. 2 provides the structural characterization of $Ni_{0.75}Cu_{0.25}(OH)_2$ (Fig. 2a) compared to the unmodified $Ni(OH)_2$ (Fig. 2b). The diffraction patterns were obtained using a multi-purpose X-ray Diffractometer D8-Advance from BRUKER AXS (Germany).

Diffraction angles of 20.024°, 32.964°, 38.43°, 51.769°, and 59.106° were observed for the $Ni_{0.75}Cu_{0.25}(OH)_2$. While the diffraction pattern shows a close fit of the Joint Committee on Powder Diffraction Standards (JCPDS) of β-$Ni(OH)_2$ (JCPDS No 00–014-0117), there is no evidence for the presence of crystalline $Cu(OH)_2$ (JCPDS No 00–013-0420). A clear shift to the right is observed for the diffraction angle at about 20°. The shift to the left at this diffraction angle (~20°) may be explained by the fact that the Cu^{2+} has an ionic radius of 0.73 Å [11] which is slightly higher than Ni^{2+} (0.72 Å). In addition, the elemental composition from ICP (0.75:0.25) and SEM/EDS (0.74: 0.26) were in agreement with the intended composition of $Ni_{0.75}Cu_{0.25}(OH)_2$.

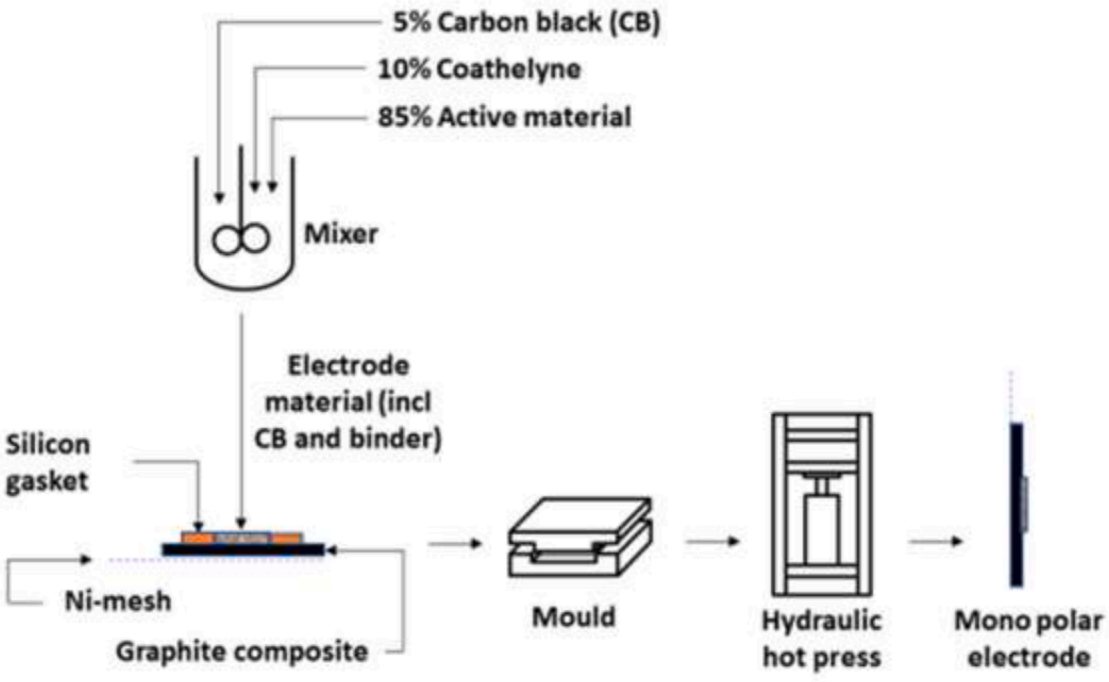

Fig. 1. Schematic illustration of the construction process flow of the Ni-based electrode production.

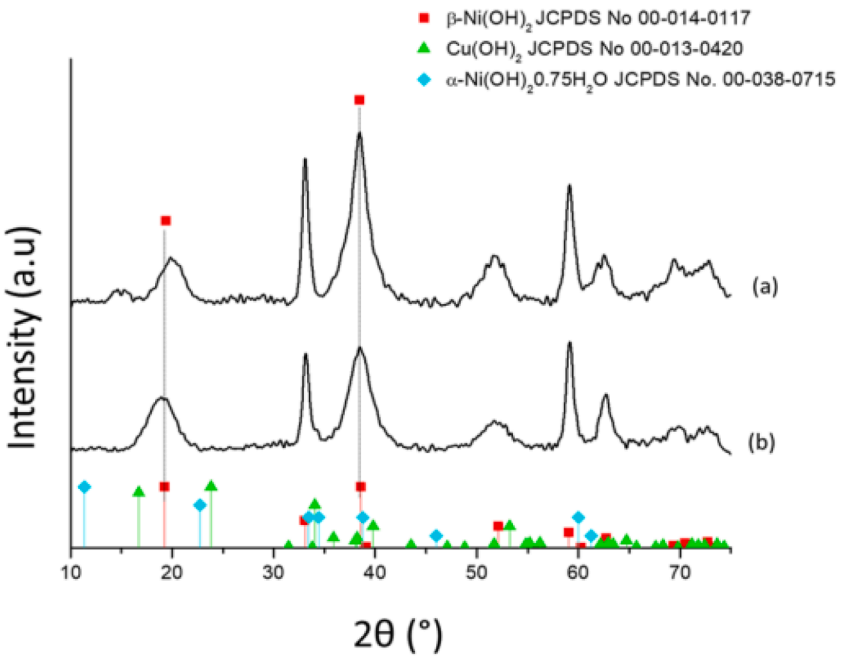

Fig. 2. Diffractogram of (a) $Ni_{0.75}Cu_{0.25}(OH)_2$ and (b) unmodified $Ni(OH)_2$.

3.2. Electrochemical characterization of $Ni_{0.75}Cu_{0.25}(OH)_2$

3.2.1. Comparison of NiFe battery cells consisting of monopolar electrodes prepared with graphite composite and Ni-mesh substrates as current collectors

Fig. 3 shows the charge-discharge curves of the battery cells prepared with the two monopolar electrode types after the 100th cycle. Two plateaus are observed, which may be represented by the reactions in Equation 1 and Equation 2 [38–40].

The reaction in Equation 1 is typically formed during the discharge of a NiFe battery cell with a negative limited configuration [38–40]. The discharge reaction (Equation 1) can further proceed in a second step (Equation 2) at a potential lower than the first step (Equation 1) [40].

Equation 1: First plateau of charge-discharge reaction of NiFe battery electrode

$$Fe + 2NiOOH + 2H_2O \underset{\text{Charge}}{\overset{\text{Discharge}}{\rightleftharpoons}} 2Ni(OH)_2 + Fe(OH)_2 \quad \text{First plateau } (Ecell = 1.37V)$$

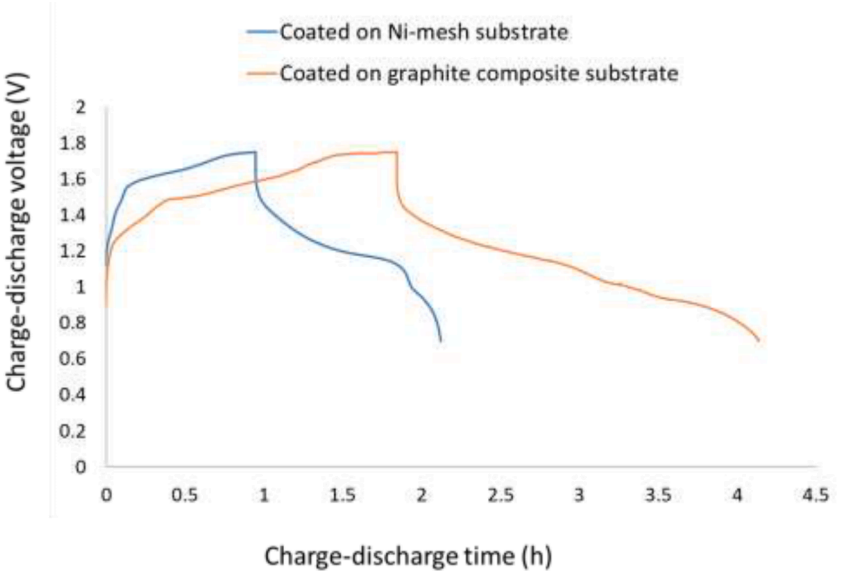

Fig. 3. Evaluation of the NiFe battery cells with monopolar- electrodes: time-voltage-current charge-discharge curves of $Ni_{0.75}Cu_{0.25}(OH)_2$ at the 100th cycle.

Equation 2: Second plateau of charge-discharge reaction of NiFe battery electrode

$$3Fe(OH)_2 + 2NiOOH \underset{\text{Charge}}{\overset{\text{Discharge}}{\rightleftharpoons}} 2Ni(OH)_2 + Fe_3O_4 + 2H_2O \text{ Second plateau } (Ecell = 1.05V)$$

During charge-discharge, the electrolyte remains fundamentally invariant and plays no part in the NiFe battery's overall reaction (Equation 3) although, the individual electrode reactions involve an intimate reaction with the electrolyte [38].

Equation 3: Overall charge-discharge reaction of NiFe battery electrode

$$3Fe + 8NiOOH + 4H_2O \underset{\text{Charge}}{\overset{\text{Discharge}}{\rightleftharpoons}} 8Ni(OH)_2 + Fe_3O_4 \text{ Overall reaction}$$

As shown in Fig. 4, constant discharge capacities were observed over the 100 cycles with no noticeable drop in discharge capacities.

The electrodes demonstrated a discharge capacity of 144 mAh/g and 199 mAh/g after the 100th cycles, corresponding to a coloumbic efficiency of 87% and 84% for monopolar electrodes with Ni-mesh and graphite substrates, respectively.

Graphite is more chemically stable compared to metals during potential cycling. Metals are known to corrode, which may lead to morphology changes that can increase interfacial contact resistance between the active material and the substrate. Additionally, metals are known to form surface oxides that lead to increased interfacial contact resistance between the active material and the substrate [41–43]. It appears that such side reactions may have contributed to the lower performances of the Ni-mesh substrate-based electrodes; however, additional experiments are required to evaluate such a claim. Thermoplastic composite bipolar plates have the advantage over metallic plates of being more resistant to chemical attack, flexible and lightweight [41–43]; however, in this study, the chemical stability is probably the main factor in improving the graphite-based cell's performance.

Table 2 summarises the test parameters and the discharge capacities obtained for the battery cells consisting of the two monopolar electrodes types after various charge-discharge cycles. The discharge capacities (over 1st cycle, 10th cycle, 50th cycle, and 100th cycle) provided in Table 2 are the obtained specific discharge capacities after the activation step (30 cycles). As evident in Table 2, the electrode fabricated on Ni-mesh showed a lower discharge capacity after the 100th cycle compared to the electrode fabricated on graphite substrate as the current collector.

3.2.2. Bipolar-based NiFe battery cell with bipolar electrode prepared with graphite substrate as the current collector

In order to develop the bipolar-based Ni-Fe battery cell, a bipolar electrode was prepared by depositing the anode material ($FeCu_{0.25}$) on one side of the graphite substrate and the cathode material (85% $Ni_{0.75}Cu_{0.25}(OH)_2$, 10% Coathylene binder, and 5% carbon black) on the other side. The bipolar-based NiFe battery cell was evaluated using a two-chamber cell (Fig. 5).

The configuration used demonstrates the design that an up-scaled bipolar Ni-Fe battery would follow. The thermoplastic graphite composite material has a much lower weight and better corrosion resistance than the Ni-mesh. Therefore, it will be utilized as the bipolar plate, which is a constituent of every cell of the bipolar battery. This will be a key factor in reducing the overall stack complexity, weight, and size of the Ni-Fe battery. The electronic conductivity of a Ni-Mesh is almost 20 times higher than the electronic conductivity of the graphite bipolar plate. In a bipolar electrode, the current only flows in the through-plane direction over a distance of 50 microns. In the endplate, the current needs to flow in the in-plane direction towards the external terminals. The ohmic resistance observed in an endplate is therefore far greater than for a central bipolar electrode.

The bipolar electrode (Fig. 6) was placed at the chamber's centre (Fig. 5), and the anodic and cathodic monopolar current collectors were positioned inside each chamber, as demonstrated in Fig. 7.

The charge-discharge cut-off voltage-limiting was kept at 3.5 V - 0.7

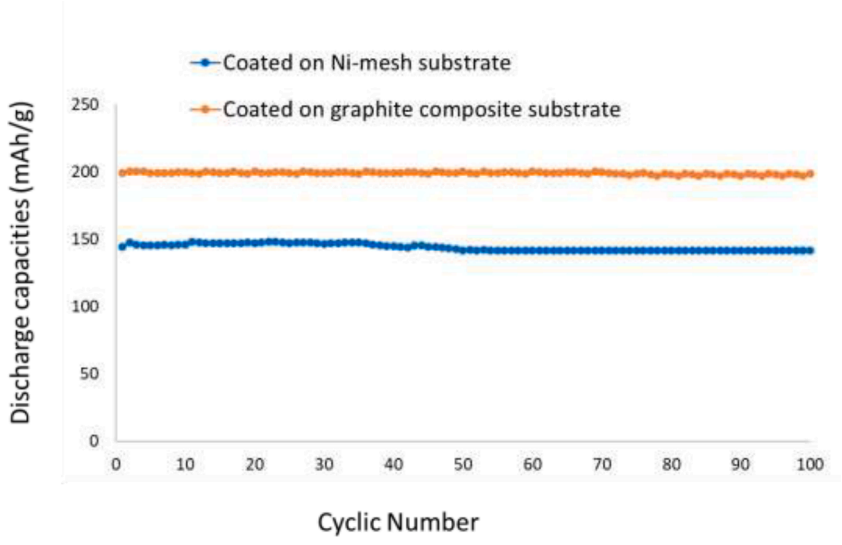

Fig. 4. Evaluation of the NiFe battery cells with monopolar- electrodes: specific discharge capacity curves over 100 cycles for $Ni_{0.75}Cu_{0.25}(OH)_2$.

Table 2
Electrochemical test specifications for the NiFe battery cells with the two monopolar electrode types.

Electrochemical test specifications	A				B			
Cathode and anode substrate	2 cm x 2 cm Ni-mesh sheet				2 cm x 2 cm graphite composite (80% Graphite, 20% Poly propylene, Fraunhofer Umsicht			
Cathode active mass loading (limited)	0.2 g $Ni_{0.75}Cu_{0.25}(OH)_2$				0.2 g $Ni_{0.75}Cu_{0.25}(OH)_2$			
Anode active mass loading	0.9 g $FeCu_{0.25}$				0.9 g $FeCu_{0.25}$			
Electrolyte	6 M KOH/1 M LiOH				6 M KOH/1 M LiOH			
The charge cut off voltage (V)	1.75 V				1.75 V			
Discharge cut off voltage (V)	0.7 V				0.7 V			
Specific CC charge and discharge current	100 mA/g				100 mA/g			
Numbers of cycles	1	10	50	100	1	10	50	100
Electrode capacity (mAh)	28.8	29.6	28.3	28.3	39.9	39.9	40.0	39.7
Specific capacity (mAh/g)	144	146	142	142	199	200	200	199
Coulombic efficiency				87%				84%

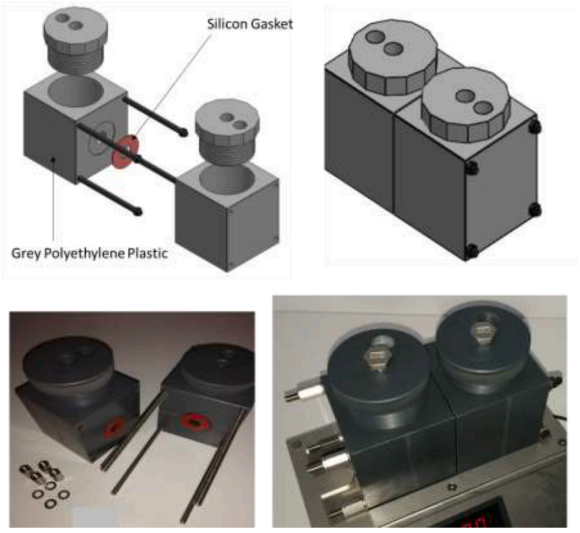

Fig. 5. Drawings and pictures of the two-chamber test cell.

V, and the cut-off current-limiting was set at 500 mA/g for both electrodes. The time-voltage charge-discharge curves of the bipolar based Ni-Fe cell at the 1st and 100th cycle is shown in Fig. 8. The presence of two plateaus may denote the reactions in Equation 1 and Equation 2 [38–40].

It is noteworthy that the activation process is a fundamental step in secondary alkaline battery technology. The electrode exhibited superlative cycling stability as it retained 88% (158 $mAhg^{-1}$) of the initial discharge capacity (180 $mAhg^{-1}$). This is attributed to the ability of Cu to lower the particle surface energy through its highly conductive network embedded in the electrode [33,44]. There were no noticeable changes in terms of plateau voltages observed between the 1st, 10th, 50th, and the 100th cycle charge-discharge profiles. However, the long-distance observed between the cycle charge-discharge profiles could be due to the differences in coulombic efficiencies, which are 51% (180 $mAhg^{-1}$), 63% (169 $mAhg^{-1}$), 70% (156 $mAhg^{-1}$), and 72% (158 $mAhg^{-1}$) for the 1st, 10th, 50th and the 100th cycle charge-discharge profiles. Therefore, 49% of the energy stored during the 1st charge cycle was wasted as only 51% was released on the 1st discharge cycle.

Fig. 9 shows the specific discharge capacity curves of the bipolar-based Ni-Fe cell after 100 cycles. Discharge capacities were observed over 100 cycles with no noticeable drop in discharge capacity after the 20th cycle (activation). The electrode demonstrated a discharge capacity of 158 mAh/g after the 100th cycle, corresponding to a coloumbic efficiency of 72% and 87% cell capacity remaining.

A summary of the test parameters and the discharge capacities obtained for the bipolar-based Ni-Fe electrode is shown in Table 3. The discharge capacities over the 1st, 10th, 50th, and 100th cycles presented in Table 3 were attained after the activation step (30 cycles).

4. Conclusion

In order to move to even thinner bipolar plates and prevent

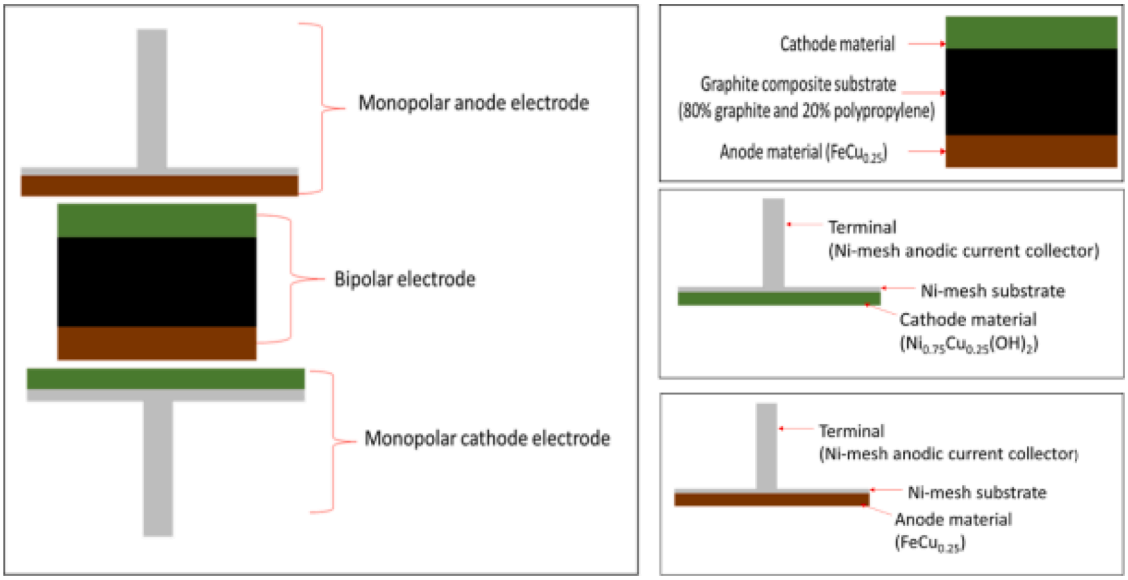

Fig. 6. Schematic representation of the construct of the bipolar based NiFe Cell.

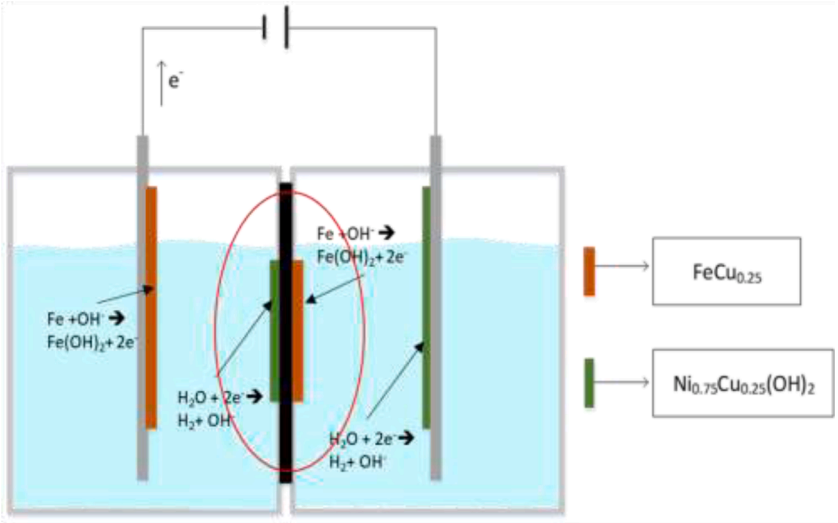

Fig. 7. Schematic diagram of a typical bipolar galvanostatic cell.

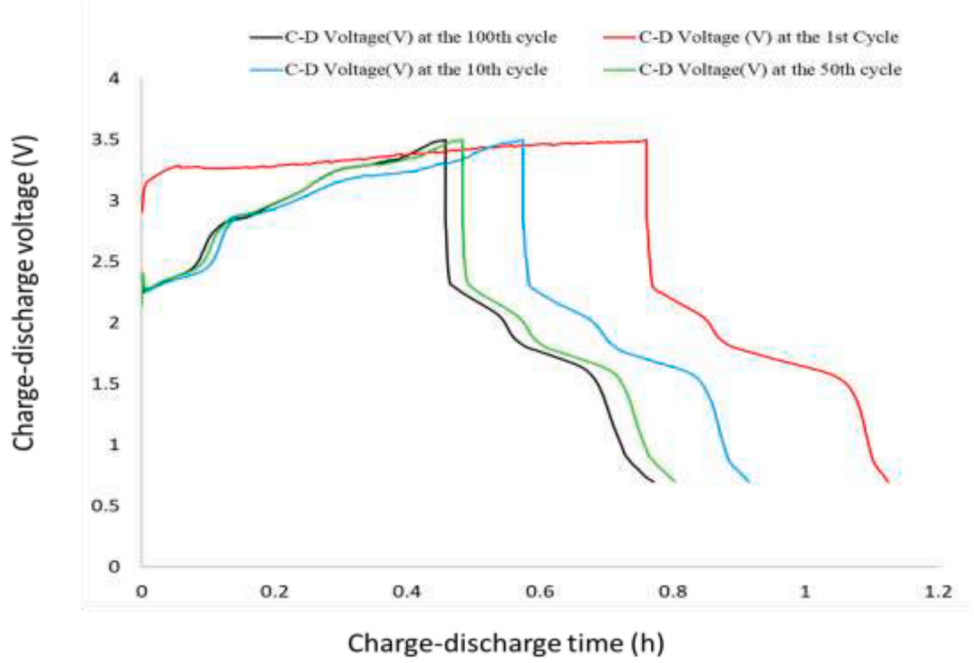

Fig. 8. Evaluation of the bipolar-based NiFe battery cell: time-voltage charge-discharge curves at the 1st, 10th, 50th, and the 100th cycle.

unacceptable mechanical strain in the electrodes, the technological challenges related to the production of reproducible bipolar electrodes need to be improved. A thermoplastic graphite composite bipolar plate consisting of graphite and polypropylene was developed and utilized in this study, which aids with the mechanical properties of the bipolar plate by increasing the flexibility and reducing the required thickness cell [41–43,45].

A novel bipolar design for the Ni-Fe battery was successfully prepared, and the preliminary results for cell discharge capacities are presented. Three NiFe battery cell types were prepared and gauged for their charge-discharge capacities. The first two cell types consisted of monopolar electrodes. One cell used the graphite composite as the current collector, and the other cell used the Ni-mesh substrates as the current collector. The third cell type consisted of a bipolar electrode prepared with a graphite substrate as the current collector coupled to two monopolar electrodes composed with Ni-mesh substrates as current collectors.

The two cells with monopolar electrodes demonstrated discharge capacities of 144 mAh/g and 199 mAh/g after the 100th cycles, corresponding to coloumbic efficiencies of 87% and 84% for the monopolar-based electrodes fabricated on Ni-mesh and graphite substrate, respectively. The bipolar-based NiFe battery two-cell demonstrated a discharge capacity of 158 mAh/g after the 100th cycle, corresponding to a coloumbic efficiency of 72%. Physical characterization such as scanning electron microscopy (SEM) and additional electrochemical characterizations such as electrochemical impedance spectroscopy and conductivity measurements of the electrodes are needed to understand the reasons for the improved discharged capacity observed when the graphite composite was used as compared to the Ni-mesh used as the current collector. The discharge capacities for bipolar NiFe cells were notably lower than the monopolar electrode using the graphite composite as the current collector. Thus, these characterizations will form part of future research to enable improvements to the bipolar NiFe battery design.

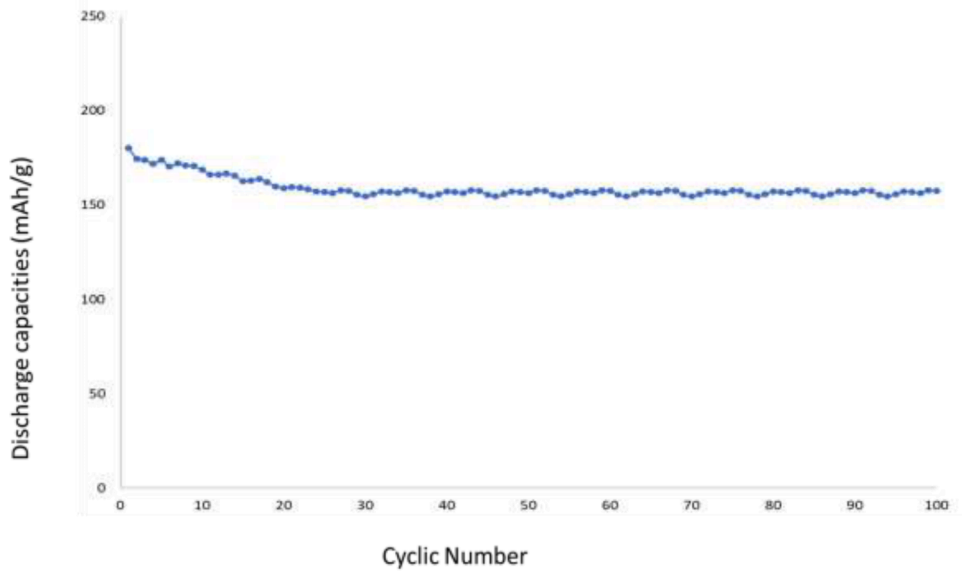

Fig. 9. Evaluation of the bipolar-based NiFe battery cell: specific discharge capacity curve over 100 cycles.

Table 3
Electrochemical test specifications for the bipolar-based NiFe cell.

Electrochemical test specifications	Bipolar cell			
Monopolar cathode / anode substrate	5 cm x 5 cm Ni-mesh sheet			
Cathode active mass loading on a monopolar electrode	1.0 g $Ni_{0.75}Cu_{0.25}(OH)_2$			
Anode active mass loading on a monopolar electrode	2.5 g $FeCu_{0.25}$			
Bipolar substrate	10 mm diameter graphite composite (80% Graphite, 20% Poly propylene, Fraunhofer Umsicht)			
The active area of the bipolar substrate	$0.8cm^2$			
Cathode active mass loading on a bipolar electrode	0.04 g $Ni_{0.75}Cu_{0.25}(OH)_2$			
Anode active mass loading on a bipolar electrode	0.08 g $Fe_{0.75}Cu_{0.25}$			
Electrolyte	6 M KOH/1 M LiOH			
The charge cut off voltage (over 2 cells effectively)	3.5 V			
Discharge cut off voltage (over 2 cells effectively)	0.7 V			
Specific CC charge and discharge current (mA/g)	500			
Numbers of cycles	1	10	50	100
Electrode capacity (mAh)	7.2	6.7	6.3	6.3
Specific capacity (mAh/g)	180	169	156	158
Coulombic efficiency	51%	63%	70%	72%

Statement of data availability

Upon a reasonable request, the data that support the finding of this study may be obtainable from the corresponding author.

Statement (Declaration) of Opposing Interest

The authors declare that they have no known competing personal relationships or financial interests that may appear to influence the work reported in this study.

CRediT authorship contribution statement

Dorcas Zide: Conceptualization, Methodology, Software, Data curation, Formal analysis, Investigation, Resources, Writing – original draft, Writing – review & editing, Supervision, Project administration. **Cecil Felix:** Writing – review & editing. **Tobie Oosthuysen:** Writing – review & editing. **Jens Burfeind:** Writing – review & editing. **Anna Grevé:** Writing – review & editing. **Bernard Jan Bladergroen:** Conceptualization, Software, Resources, Writing – review & editing, Supervision.

Declaration of Competing Interest

The authors declare that they have no known competing financial interests or personal relationships that could have appeared to influence the work reported in this paper.

Acknowledgments

The South African authors acknowledge the financial and strategic support from the Department of Science and Innovation of South Africa; Eskom Holdings SOC Ltd Reg no 2002/015527/30 (Eskom Research, Testing, and Development Business Unit); the National Research Foundation of South Africa (Grant Numbers: 121413,130409), in Germany the authors acknowledge the BMBF founding organization within the CLIENT II initiative. The project is granted under the following number: FKZ 01LZ1715A-B.

References

[1] P.G. Bruce, Promising electrochemical systems for rechargeable batteries, J. Electroanal. Chem. 421 (1997) 222–223.
[2] T. Liu, Y. Yuan, X. Tao, Z. Lin, J. Lu, Bipolar electrodes for next-generation rechargeable batteries, Adv. Sci. 7 (2020), 2001207.
[3] S. Chang, K.-h. Young, J. Nei, C. Fierro, Reviews on the US Patents regarding nickel/metal hydride batteries, Batteries 2 (2016) 10.
[4] S.H. Kim, J.H. Kim, S.J. Cho, S.Y. Lee, All-solid-state printed bipolar Li-S batteries, Adv. Energy Mater. 9 (2019), 1901841.
[5] E. Peled, D. Golodnitsky, G. Ardel, J. Lang, Y. Lavi, Development and characterization of bipolar lithium composite polymer electrolyte (CPE)-FeS_2 battery for applications in electric vehicles, Power Sources 54 (1995) 496–500.
[6] M. Alamgir, K. Abraham, Room temperature rechargeable polymer electrolyte batteries, Power Sources 54 (1995) 40–45.
[7] T. Liu, Y. Zhang, C. Chen, Z. Lin, S. Zhang, J. Lu, Sustainability-inspired cell design for a fully recyclable sodium ion battery, J. Nat. Commun. 10 (2019) 1–7.
[8] S. Ullah, F.A. Amin Badshah, R. Raza, A.A. Altaf, and R. Hussain, "Electrodeposited zinc electrodes for high current Zn/AgO bipolar batteries," 2011.
[9] M. Rota, C. Comninellis, S. Moller, F. Holzer, O. Haas, Bipolar Al/O_2 battery with planar electrodes in alkaline and acidic electrolytes, Appl. Electrochem. 25 (1995) 114–121.
[10] S. Müller, F. Holzer, O. Haas, C. Schlatter, C. Comninellis, Development of rechargeable monopolar and bipolar zinc/air batteries, CHIMIA Int. J. Chem. 49 (1995) 27–32.
[11] V. Livshits, A. Blum, E. Strauss, G. Ardel, D. Golodnitsky, E. Peled, Development of a bipolar Li/composite polymer electrolyte/pyrite battery for electric vehicles, Power Sources 97 (2001) 782–785.

[12] Y. Gambe, Y. Sun, I. Honma, Development of bipolar all-solid-state lithium battery based on quasi-solid-state electrolyte containing tetraglyme-LiTFSA equimolar complex, Sci. Rep. 5 (2015) 1–4.
[13] J. Janek, W.G. Zeier, A solid future for battery development, Nat. Energy 1 (2016) 1–4.
[14] K.N. Jung, H.S. Shin, M.S. Park, J.W. Lee, Solid-state lithium batteries: bipolar design, fabrication, and electrochemistry, ChemElectroChem 6 (2019) 3842–3859.
[15] J. Yan, Q. Wang, T. Wei, Z. Fan, Recent advances in design and fabrication of electrochemical supercapacitors with high energy densities, Adv. Energy Mater. 4 (2014), 1300816.
[16] S. Gheytani, Y. Liang, Y. Jing, J.Q. Xu, Y. Yao, Chromate conversion coated aluminium as a light-weight and corrosion-resistant current collector for aqueous lithium-ion batteries, J. Mater. Chem. A 4 (2016) 395–399.
[17] Y. Yamada, K. Usui, K. Sodeyama, S. Ko, Y. Tateyama, A. Yamada, Hydrate-melt electrolytes for high-energy-density aqueous batteries, Nat. Energy 1 (2016) 1–9.
[18] X. Zhou, C. Peng, G.Z. Chen, 20V stack of aqueous supercapacitors with carbon (−), titanium bipolar plates and CNT-polypyrrole composite (+), AIChE J. 58 (2012) 974–983.
[19] K.C. Ng, S. Zhang, C. Peng, G.Z. Chen, Individual and bipolarly stacked asymmetrical aqueous supercapacitors of CNTs/SnO_2 and CNTs/MnO_2 nanocomposites, J Electrochem. Soc. 156 (2009) A846.
[20] W. Zuo, R. Li, C. Zhou, Y. Li, J. Xia, J. Liu, Battery-supercapacitor hybrid devices: recent progress and future prospects, Adv. Sci. 4 (2017), 1600539.
[21] H.C. Wu, Y.P. Lin, E. Lee, W.T. Lin, J.K. Hu, H.C. Chen, N.L. Wu, High-performance carbon-based supercapacitors using Al current-collector with conformal carbon coating, Mater. Chem. Phys. 117 (2009) 294–300.
[22] M.R. Lukatskaya, S. Kota, Z. Lin, M.Q. Zhao, N. Shpigel, M.D. Levi, J. Halim, P. L. Taberna, M.W. Barsoum, P. Simon, Ultra-high-rate pseudocapacitive energy storage in two-dimensional transition metal carbides, Nat. Energy 2 (2017) 1–6.
[23] J. Whitacre, T. Wiley, S. Shanbhag, Y. Wenzhuo, A. Mohamed, S. Chun, E. Weber, D. Blackwood, E. Lynch-Bell, J. Gulakowski, An aqueous electrolyte, sodium ion functional, large format energy storage device for stationary applications, Power Sources 213 (2012) 255–264.
[24] B. Ziv, O. Haik, E. Zinigrad, M.D. Levi, D. Aurbach, I.C. Halalay, Investigation of graphite foil as current collector for positive electrodes of Li-ion batteries, J Electrochem. Soc. 160 (2013) A581.
[25] B. Dyatkin, V. Presser, M. Heon, M.R. Lukatskaya, M. Beidaghi, Y. Gogotsi, Development of a green supercapacitor composed entirely of environmentally friendly materials, ChemSusChem 6 (2013) 2269–2280.
[26] N. Blomquist, T. Wells, B. Andres, J. Bäckström, S. Forsberg, H. Olin, Metal-free supercapacitor with aqueous electrolyte and low-cost carbon materials, Sci. Rep. 7 (2017) 1–7.
[27] D.H. Shen, G. Halpert, Design concepts of high power bipolar rechargeable lithium battery, Power Sources 43 (1993) 327–338.
[28] H. Karami, M.F. Mousavi, M. Shamsipur, A novel dry bipolar rechargeable battery based on polyaniline, Power Sources 124 (2003) 303–308.
[29] K. Yoshima, Y. Harada, N. Takami, Thin hybrid electrolyte based on garnet-type lithium-ion conductor $Li7La_3Zr_2O_{12}$ for 12V-class bipolar batteries, Power Sources 302 (2016) 283–290.
[30] A.H. Abdalla, C.I. Oseghale, J.O.G. Posada, P.J. Hall, Rechargeable nickel-iron batteries for large-scale energy storage, Inst. Eng. Technol. Renew. Power Gener. 10 (2016) 1529–1534.
[31] J.O.G. Posada, P.J. Hall, Towards the development of safe and commercially viable nickel-iron batteries: improvements to coulombic efficiency at high iron sulphide electrode formulations, Appl. Electrochem. 46 (2016) 451–458.
[32] W. Chen, Y. Jin, J. Zhao, N. Liu, Y. Cui, Nickel-hydrogen batteries for large-scale energy storage, Proc. Natl. Acad. Sci. 115 (2018) 11694–11699.
[33] T. Tawonezvi, B.J. Bladergroen, J. John, Development of $FeCu_x$/FeS/Graphite composite electrode materials for iron-based Alkaline batteries, Int. J. Electrochem. Sci. 15 (2020) 12428–12446.
[34] D. Zide, C. Felix, T. Oosthuysen, B.J. Bladergroen, Electrochemical studies of the nickel-based hydroxide electrode for the oxygen evolution reaction and coulombic efficiency of the electrode, Electroanalysis 32 (2020) 2703–2712.
[35] D. Zide, C. Felix, T. Oosthuysen, B.J. Bladergroen, The influence of copper and carbon black on electrochemical behavior of nickel positive electrode, J. Electroanal. Chem. 878 (2020), 114539.
[36] D. Zide, C. Felix, T. Oosthuysen, B.J. Bladergroen, Synthesis, structural characterization, and electrochemical properties of the Mg and Mn doped-Ni (OH) 2 for use as active cathode materials in NiFe batteries, J. Electroanal. Chem. 895 (2021), 115418.
[37] L. Kopietz, J. Girschik, P. Schwerdt, J. Burfeind, A. Grevé, C. Doetsch, Highly flexible bipolar plates for redox-flow-batteries, in: Proceedings of the Presented at the International Conference on Carbon Materials and Technology, Fraunhofer Institute for Environmental, Safety, and Energy Technology Umsicht, 2018.
[38] P.J. Tsais, L. Chan, Nickel-based batteries: materials and chemistry. Electricity Transmission, Distribution and Storage Systems, Elsevier, 2013, pp. 309–397.
[39] H. Wang, Y. Liang, M. Gong, Y. Li, W. Chang, T. Mefford, J. Zhou, J. Wang, T. Regier, F. Wei, An ultrafast nickel–iron battery from strongly coupled inorganic nanoparticle/nanocarbon hybrid materials, J. Nat. Commun. 3 (2012) 917.
[40] B. Hariprakash, S. Martha, M. Hegde, A. Shukla, A sealed, starved-electrolyte nickel–iron battery, Appl. Electrochem. 35 (2005) 27–32.
[41] R. Yeetsorn, M.W. Fowler, C. Tzoganakis, A review of thermoplastic composites for bipolar plate materials in PEM fuel cells, Nanocompos. Unique Prop. Appl. Med. Ind. (2011) 317–344.
[42] H. Fatima, Y. Zhong, H. Wu, Z. Shao, Recent advances in functional oxides for high energy density sodium-ion batteries, Mater. Rep. Energy (2021), 100022.
[43] Y. Zhong, X. Xu, J.P. Veder, Z. Shao, Self-recovery chemistry and cobalt-catalyzed electrochemical deposition of cathode for boosting performance of aqueous zinc-ion batteries, Iscience 23 (2020), 100943.
[44] L. Huang, J. Yang, P. Liu, D. Zhu, Y. Chen, Copper/iron composite anode prepared by *in situ* co-precipitation with excellent high-rate and low-temperature performance for rechargeable nickel-iron battery, Int. J. Electrochem. Sci. 13 (2018) 7045–7056.
[45] Y. Zhong, X. Xu, Y. Liu, W. Wang, Z. Shao, Recent progress in metal–organic frameworks for lithium–sulfur batteries, Polyhedron 155 (2018) 464–484.